Int J Thermophys (2008) 29:546–556
DOI 10.1007/s10765-007-0369-6

Thermodynamic Properties of HFC-236ea

V. A. Gruzdev · R. A. Khairulin · S. G. Komarov · S. V. Stankus

Received: 29 March 2006 / Accepted: 27 December 2007 / Published online: 29 January 2008

Abstract The density of gaseous and liquid 1,1,1,2,3,3-hexafluoropropane (HFC-236ea) and the speed of sound in liquid HFC-236ea have been studied by a γ-attenuation technique, an ultrasonic interferometer, and an isochoric piezometer method over the temperature range of 263–423 K at pressures up to 4.05 MPa. The purity of the samples used throughout the measurements is 99.68 mol%. The pressures of the saturated vapor were measured over the same temperature range. The experimental uncertainties of the temperature, pressure, density, and speed-of-sound measurements were estimated to be within ±20 mK, ±1.5 kPa, ±(0.05–0.30)%, and ±(0.05–0.10)%, respectively.

Keywords Density · Gamma densimeter · HFC-236ea · Isochoric piezometer · Speed of sound · Ultrasonic interferometer · Vapor pressure

1 Introduction

Thermal properties of 1,1,1,2,3,3-hexafluoropropane (HFC-236ea) have been studied for the most part in the range up to 390 K and 1.6 MPa [1–4]. Moreover, density and speed-of-sound measurements have been carried out by comparative methods. In the present paper, we report measurements for the density of liquid and gaseous 1,1,1,2,3,3-hexafluoropropane, for the vapor pressure of HFC-236ea, and for the speed of sound in liquid HFC-236ea over the temperature range of 263–423 K and at pressures up to 3.0–4.05 MPa. The purity of the samples used throughout the measurements was 99.68 mol%.

V. A. Gruzdev · R. A. Khairulin · S. G. Komarov · S. V. Stankus (✉)
Institute of Thermophysics, Siberian Branch of the Russian Academy of Sciences,
Lavrentyev Ave., 1, Novosibirsk 630090, Russia
e-mail: stankus@itp.nsc.ru

2 Experimental

The methods used for measurement of the thermal properties have been described in previous publications [5–7]. The saturated vapor pressure (P_S) and the density (ρ_v) of the superheated vapor were measured with an isochoric piezometer of 439.35 cm^3 capacity. The cell was immersed in a thermostatic bath. The temperature in the bath was held to within ±5 mK throughout the measurements. The temperature of the piezometer was measured on ITS-90 with a 50-Ω platinum resistance thermometer calibrated at the Siberian Scientific Research Institute of Metrology, Novosibirsk. The uncertainty in the temperature measurement was estimated to be ±0.02 K. Instrumental error in the pressure measurement in the range up to 0.6 MPa did not exceed 0.3 kPa, and at 4 MPa it was about 3 kPa. The main contribution to the uncertainty of the vapor-density determination gives an uncertainty in the sample mass which was 0.05–0.15% at densities above 100 $kg \cdot m^{-3}$ and 0.3% at 12 $kg \cdot m^{-3}$.

The investigation of the density in the liquid state was performed by irradiating the samples with a narrow beam of gamma quanta from the ^{137}Cs source (220 GBq). The basic advantages of this method are it is contact free and universal. The lifting gear allows for vertical movement of the installation with respect to the beam and thus to measure the gamma-ray attenuation in the sample in relation to the distance from the cell bottom (h). This makes it possible for concurrent measurements of the densities of two equilibrium phases along the coexistence curve. To estimate unaccounted for systematic errors, we measured the density of distilled deaerated water. These experiments have shown that the experimental uncertainties of the liquid and vapor densities are within ±(1–1.5) $kg \cdot m^{-3}$ over the temperature range from 293 to 523 K [7].

The speed of sound was measured by an ultrasonic interferometer with variations in the distance between the transducer and transmitter. The interferometer was fabricated from stainless steel with lithium niobate transducers operated at a frequency close to 1 MHz. Instrumental errors of the pressure and temperature measurements were the same as in the vapor-density experiments. To estimate the instrumental error in the measurements of the speed of sound, we made performance test measurements in pure argon. The results obtained during these experiments differ from the most reliable data by no more than 0.06%.

The purity of the HFC-236ea sample used in the present measurements was 99.68 mol%. The main impurity was HFC-245 (0.3 mol%). Before the experiments were initiated, the initial product was purified by removing water and volatile components [5].

3 Results and Discussion

3.1 Saturated Vapor Pressure

The results of measurements of the saturated vapor pressure are given in Table 1. The experimental data were fitted with an empirical equation for the liquid–vapor equilibrium curve:

Table 1 Experimental vapor pressures of HFC-236ea

T (K)	P (kPa)	T (K)	P(kPa)	T (K)	P (kPa)
293.15	172.4	343.16	783.2	391.15	2274.8
294.08	178.0	350.15	932.0	393.15	2362.0
298.15	206.0	353.15	1000.8	393.15	2364.9
303.15	244.2	353.15	999.6	398.15	2605.2
308.15	288.0	363.15	1263.5	403.15	2874.5
313.15	337.2	363.15	1262.7	403.15	2871.5
313.15	337.5	372.15	1537.2	408.15	3145.8
318.15	392.6	373.15	1569.7	408.75	3197.6
323.15	455.2	373.15	1570.9	411.08	3336.0
333.15	602.0	381.15	1860.2	412.15	3397.2
333.15	602.5	383.15	1935.9		

$$\ln\left(\frac{P_S}{P_0}\right) = \left(C_1\varepsilon + C_2\varepsilon^{1.5} + C_3\varepsilon^{2.5} + C_4\varepsilon^{6}\right)\frac{T_C}{T} \tag{1}$$

where $C_1 = -7.948537$, $C_2 = 2.1579416$, $C_3 = -3.503473$, $C_4 = -5.605665$, $\varepsilon = 1 - T/T_C$, $T_C = 412.375\,\mathrm{K}$ is the critical temperature [3], and $P_0 = P(T_C) = 3416.95\,\mathrm{kPa}$. Equation 1 describes the experimental data with a standard deviation of 0.09% in the temperature range from 293.15 to 412.15 K. Deviations of our experimental data, as well as literature results [1,3,4], from Eq. 1 are shown in Fig. 1. As seen from the figure, our data are in good agreement with the most reliable results [3]. The data of Zhang et al. [3] lie about 0.05% higher at 293 K and about 0.10% higher at 400 K. Deviations for other sets of data at this temperature are 0.4–0.5%. The normal boiling temperature $T_b = 279.31 \pm 0.2\,\mathrm{K}$ was determined by extrapolating Eq. 1 to atmospheric pressure (101.325 kPa).

3.2 Vapor Densities

PVT properties of HFC-236ea in the gaseous phase were measured on 14 quasi-isochores (at constant mass of the substance in the piezometer) over the density range from $12.03\,\mathrm{kg\cdot m^{-3}}$ to $501.8\,\mathrm{kg\cdot m^{-3}}$ and the temperature range from the saturation line to 423 K. The uncertainties of the temperature, pressure, and density did not exceed ± 0.02 K, 0.15%, and $\pm(0.05$–$0.30)$%, respectively. *PT* relations along isochors are given in Table 2. Corrections due to thermal expansion and pressure deformation of the piezometer do not exceed ± 0.2%. The values of the second virial coefficients $B_2(T)$ were determined by approximation of the *PVT* isotherms in the range of densities less than $106.7\,\mathrm{kg\cdot m^{-3}}$. Errors in determining B_2 at temperatures above 340 K did not exceed 2–3%. Comparison of our data for B_2 with the results of other researchers is shown in Fig. 2. The temperature dependences of B_2 for HFC-227ea [5, 8] and propane [9] are also given. Since the molecules of R-227ea and R-236ea have considerable

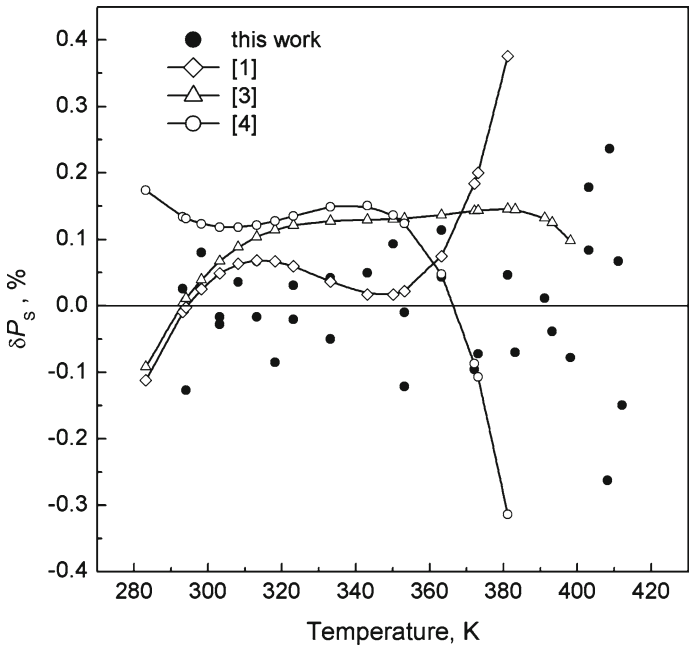

Fig. 1 Deviations of the saturated vapor pressure from Eq. 1 as a function of temperature: $\Delta P_S = [P_S(\text{Ref.})/P_S\ (\text{Eq. 1}) - 1] \times 100\%$

dipole moments, their B_2 values are much less than those for propane. The obtained data for B_2 are represented by a power series with respect to reciprocal temperature,

$$B_2(T) = b_0 + \frac{b_1}{T_r} + \frac{b_2}{T_r^2} + \frac{b_3}{T_r^3} \tag{2}$$

where $T_r = T/412.375, b_0 = 0.063198, b_1 = 0.005592, b_2 = -0.24125$, and $b_3 = -0.14984$. The *PVT* data calculated by using the second and third virial coefficients from Refs. [1] and [3] give values a little lower than our results. Deviations with data from Defibaugh et al. [1] up to 363 K are less than the experimental errors; however, they increase at higher temperatures. Discrepancies with the data of Zhang et al. [3] are up to −0.9 to −1% at a vapor density greater than $106.7\,\text{kg}\cdot\text{m}^{-3}$.

3.3 Liquid Densities

The liquid density (ρ_l) was measured along four isotherms from 300 to 374 K at pressures from the saturation line to 3.2 MPa. The experimental data for each isotherm were fitted by the equation,

$$\rho_l = C_0 + C_1 P + C_2 P^2 \tag{3}$$

Table 2 Experimental *PVT* data in gaseous HFC-236ea

T (K)	P(kPa)	T(K)	P (kPa)	T(K)	P (kPa)
$\rho_v = 12.026\,kg\cdot m^{-3}$		383.15	816.36	405.65	2766.1
313.15	194.49	393.15	845.24	408.15	2819.0
323.15	201.80	403.15	873.62	410.65	2872.0
343.15	216.06	413.15	901.67	413.15	2924.5
363.15	230.21	423.15	929.58	415.65	2975.8
383.15	244.36	$\rho_v = 61.019\,kg\cdot m^{-3}$		418.15	3027.2
403.15	258.22	383.15	1080.9	420.65	3078.6
423.15	272.00	393.15	1123.0	423.15	3130.0
$\rho_v = 15.336\,kg\cdot m^{-3}$		403.15	1164.9	$\rho_v = 238.93\,kg\cdot m^{-3}$	
303.15	234.57	413.15	1205.9	400.64	2734.8
313.15	244.25	423.15	1246.9	403.15	2794.9
323.15	253.54	$\rho_v = 81.424\,kg\cdot m^{-3}$		408.15	2916.3
333.15	263.00	362.15	1224.7	413.15	3035.6
343.15	272.14	363.15	1231.2	418.15	3152.4
353.15	281.27	368.15	1262.8	423.15	3268.2
373.15	299.63	373.15	1291.6	$\rho_v = 305.22\,kg\cdot m^{-3}$	
383.15	308.68	383.15	1356.3	413.15	3285.9
393.15	317.58	393.15	1416.6	413.15	3285.4
403.15	326.48	403.15	1475.5	417.15	3413.4
413.15	335.28	413.15	1533.4	419.15	3477.1
423.15	341.11	423.15	1591.4	419.15	3477.0
$\rho_v = 22.772\,kg\cdot m^{-3}$		$\rho_v = 106.72\,kg\cdot m^{-3}$		423.15	3603.5
316.15	354.27	383.15	1643.7	$\rho_v = 375.42\,kg\cdot m^{-3}$	
318.15	358.97	393.15	1729.6	413.15	3398.7
323.15	364.12	403.15	1813.8	418.15	3616.7
333.15	378.59	413.15	1895.9	423.15	3822.7
343.15	392.89	423.15	1977.6	$\rho_v = 421.82\,kg\cdot m^{-3}$	
353.15	407.01	$\rho_v = 172.61\,kg\cdot m^{-3}$		414.98	3533.4
363.15	420.93	390.36	2239.4	417.15	3639.3
373.15	434.79	393.15	2285.4	419.15	3735.8
383.15	448.58	398.15	2367.3	421.15	3832.3
393.15	462.31	403.15	2447.1	423.15	3928.4
403.15	475.88	408.15	2525.7	$\rho_v = 501.79\,kg\cdot m^{-3}$	
423.15	502.99	413.15	2602.9	415.15	3580.6
$\rho_v = 43.840\,kg\cdot m^{-3}$		418.15	2678.6	417.13	3696.0
343.15	697.68	423.15	2754.2	419.06	3809.5
353.15	727.92	$\rho_v = 218.65\,kg\cdot m^{-3}$		419.48	3834.6
363.15	757.83	401.15	2339.1	421.15	3931.4
373.15	787.41	403.15	2711.9	423.15	4048.7

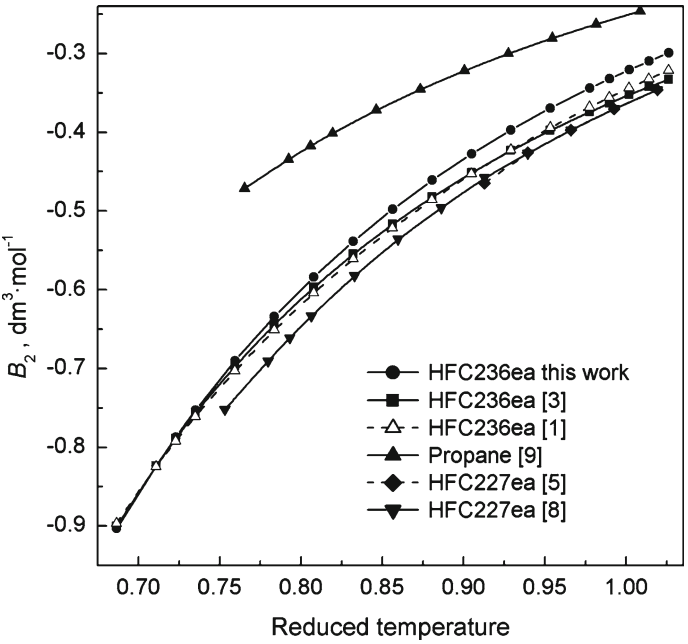

Fig. 2 Temperature dependence of the second virial coefficients for propane and its fluorinated derivatives

Table 3 Parameters of Eq. 3

T (K)	C_0	C_1	C_2
303.91	1402.83	6.0064	−0.49945
323.94	1331.58	6.23406	−0.13905
353.89	1202.15	14.2429	−0.80003
373.99	1074.33	29.0995	−2.28183

where ρ_l (kg · m^{-3}) is the liquid density and P is the pressure (MPa). The values of the coefficients of Eq. 3 are given in Table 3. The standard deviations of experimental points do not exceed ±0.075%, which is in good agreement with the estimated uncertainty of density measurements using the gamma method. At the same time, systematic deviations of our results from Defibaugh et al. [1] (∼0.4%) obtained by a vibrating method are observed. This discrepancy is larger than the estimated uncertainties of both methods.

3.4 Densities of Vapor and Liquid on Saturation Line

The vapor (ρ_v^S) and liquid densities (ρ_l^S) on the saturation line were measured by the gamma method from 299 to 411.95 K (Figs. 3 and 4) and were also obtained by extrapolation of the experimental data for the vapor density from the superheated state to the saturation line (Table 4). As already noted, the gamma densimeter can be used for measurements of the height dependence of the density of a two-phase sample.

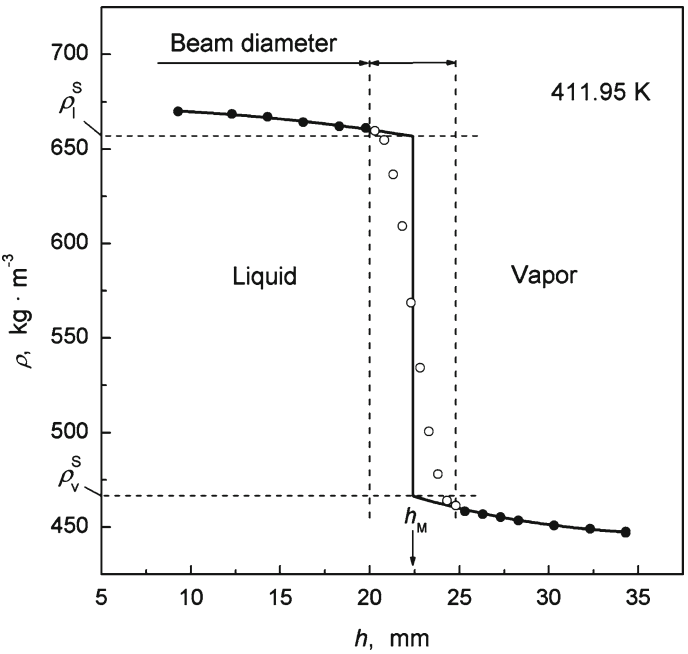

Fig. 3 Height dependence of the density of two-phase sample of HFC-236ea at 411.95 K. Solid and open circles are experimental data. h_M is the interface location. Solid line represents real density profile derived from the procedure, which is described in the main text. ρ_l^S and ρ_v^S shows the densities of the liquid and vapor phases in equilibrium

This makes it possible to observe the so-called hydrostatic (or gravitational) effect connected with the high compressibility near the critical point of the liquid–vapor coexistence curve. The effect manifests itself in that densities of the phases become height dependent when the temperature is close to the critical value. This phenomenon was observed at temperatures above 411 K; see Fig. 3 and Table 5. To determine the densities of the liquid and vapor in equilibrium with each other, we must extrapolate to the two-phase interface. On the other hand, since the diameter of the gamma-ray beam is 4.4 mm, the stepwise density change occurring in passing through the interface appears as a continuous transition taking place in the height interval equal to the beam width (open circles in Fig. 3). The following procedure was used for determination of the meniscus location, h_M, and the densities of the equilibrium phases. The observed density profile over the region of its drastic change was fitted with a polynomial. It can be easily shown that the $d\rho/dh$ derivative has a maximum value when the axis of the gamma-ray beam passes through the phase boundary. This distance was taken as the meniscus location, h_M. The densities of the liquid (ρ_l^S) and vapor (ρ_v^S) phases in equilibrium with each other were determined by extrapolation of the approximate height dependences of the liquid $\rho_l(h)$ and vapor $\rho_v(h)$ densities (solid lines in Fig. 3) to h_M.

The asymptotic behavior of the liquid–vapor coexistence curve in the vicinity of the critical point is described by [10]

$$\left(\rho_l^S - \rho_v^S\right) = A\varepsilon^\beta \tag{4}$$

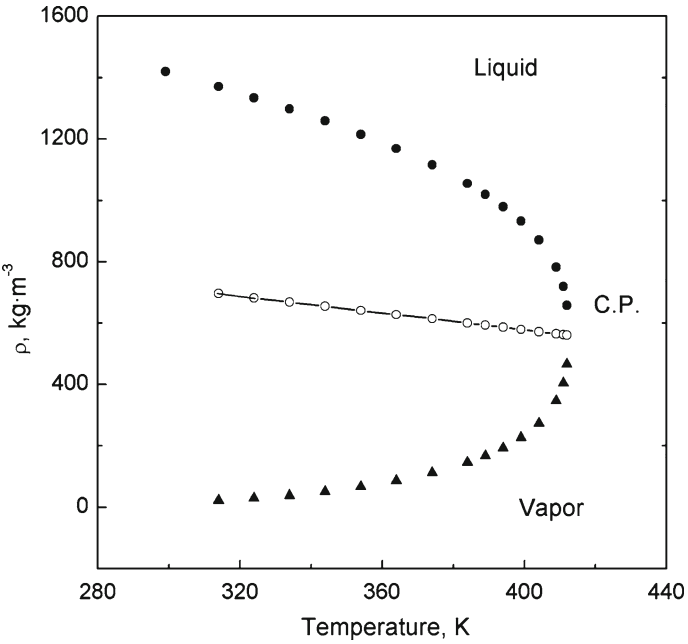

Fig. 4 Orthobaric densities of HFC-236ea along the liquid – vapor equilibrium line. Solid circles and triangles are the experimental points for liquid and vapor phases, respectively. Open circles are the midpoints of the coexistence curve

Here, $\varepsilon = 1 - T/T_C$, T_C is the critical temperature, A is a constant, and β is the critical exponent of the coexistence curve. To determine β and T_C, data for the density (Table 4) over the ε range from 2.9×10^{-3} to 0.27 were fitted by Eq. 4. The obtained values are $T_C = 412.21 \pm 0.05$ K and $\beta = 0.332 \pm 0.005$. The critical exponent, β, is close to the non-classical value of β calculated from the Ising model; according to various methods, the calculated value lies in the range from 0.31 to 0.34 [10]. To determine the critical density ρ_C, experimental data were fitted by the equation [10],

$$(\rho_l + \rho_v)/2 = \rho_C + D_1\varepsilon^{1-\alpha} + D_2\varepsilon \tag{5}$$

where $\alpha = 0.11$ is the critical exponent for the heat capacity, $D_1 = 82.05407921$, $D_2 = 471.75471253$, and $\rho_C = 560 \pm 2\,\mathrm{kg\cdot m^{-3}}$. This value is in good agreement with $\rho_C = 563 \pm 3\,\mathrm{kg\cdot m^{-3}}$ [1] The data for the density of the liquid and vapor phases along the coexistence curve obtained by the gamma method were fitted by the following equation [5]:

$$\rho_{l,v}^S = 560(1 + C_1\varepsilon^{0.332} + C_2\varepsilon + C_3\varepsilon^{2/3} + C_4\varepsilon^{4/3}) \tag{6}$$

where $C_1 = -1.92637581$, $C_2 = 0.60310899$, $C_3 = -0.07888106$, and $C_4 = 0.82511125$ for the vapor phase and $C_1 = 1.87155509$, $C_2 = 0.05435007$, $C_3 = 0.62854123$, and $C_4 = 0.20244298$ for the liquid phase. Equation 6 describes the

Table 4 Liquid and vapor densities of HFC-236ea on the saturation line

Gamma densimeter			Isochoric piezometer[a]	
T (K)	ρ_l^S (kg·m^{-3})	ρ_v^S (kg·m^{-3})	T (K)	ρ_v^S (kg·m^{-3})
299.06	1419.9	–	294.49	12.03
313.98	–	21.29	301.79	15.34
313.99	1370.9	21.79	314.51	22.77
313.99	–	22.19	337.77	43.84
314.02	–	21.39	350.36	61.01
323.94	1334.2	29.02	350.39	61.01
333.93	1297.6	38.66	361.73	81.42
343.94	1258.4	50.72	372.40	106.7
354.04	1215.2	66.48	372.50	106.7
364.00	1168.8	86.37	390.36	172.6
374.09	1115.9	112.2	398.06	218.7
384.01	1054.3	145.8	400.58	238.9
389.01	1018.7	167.6	400.62	238.9
394.04	978.8	193.5	410.23	375.4
399.06	931.5	227.3		
404.12	870.6	273.5		
409.01	782.6	346.8		
411.00	719.3	404.5		
411.95	656.8	466.3		

[a] Data are obtained by extrapolation of the superheated vapor isochores to the saturation line

Table 5 Height dependence of the density of two-phase sample of HFC-236ea at 411.95 K

h (mm)	Phase	ρ (kg·m^{-3})	h (mm)	Phase	ρ (kg·m^{-3})
9.3	Liquid	670.0	23.3	Two phases	500.7[a]
12.3		668.6	23.8		478.0[a]
14.3		667.1	24.3		464.1[a]
16.3		664.2	24.8		461.4[a]
18.3		662.0	25.3	Vapor	458.3
19.8		661.2	26.3		456.9
20.3	Two phases	659.7[a]	27.3		455.3
20.8		654.9[a]	28.3		453.5
21.3		636.6[a]	30.3		450.9
21.8		609.2[a]	32.3		449.1
22.3		568.7[a]	34.3		447.7
22.8		534.2[a]	34.3		446.9

[a] Effective density (see caption to Fig. 3)

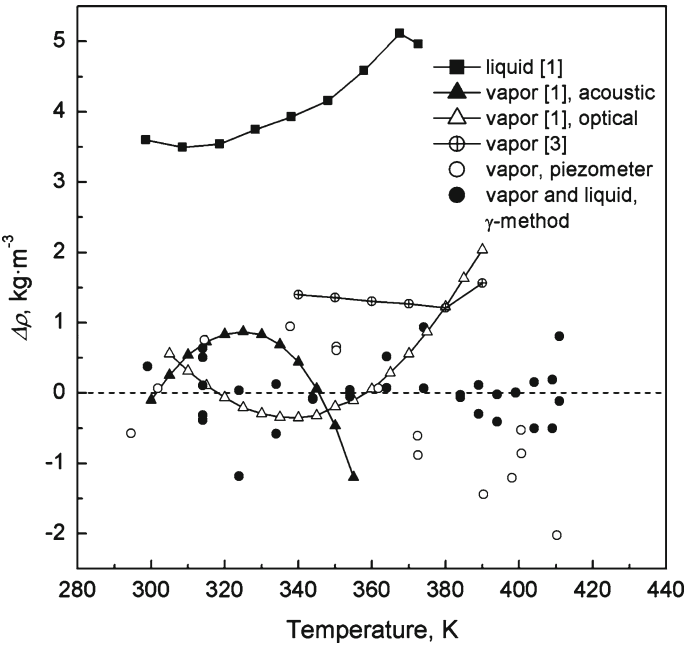

Fig. 5 Deviations of the saturated vapor and liquid density from Eq. 6 as a function of temperature; solid circles are our data obtained by the γ-method, open circles are our data obtained by the isochoric piezometer method: $\Delta\rho = \rho^{S}_{l,v}$ (Ref.) $- \rho^{S}_{l,v}$ (Eq. 6)

Table 6 Experimental sound speeds in liquid HFC-236ea

T (K)	P (kPa)	U(m·s^{-1})	P (kPa)	U(m·s^{-1})	P (kPa)	U(m·s^{-1})	P (kPa)	U(m·s^{-1})
263.15	49.75	731.68	68.24	731.18	2456.6	746.18	2423.3	745.79
273.15	77.80	690.8	78.27	689.15	138.04	689.2	1030.4	695.69
273.15	1032.8	696.07	2778.1	706.74				
283.15	121.32	646.39	179.50	648.10	1466.4	657.74	1474.8	656.88
283.15	2291.9	664.66	2312.53	664.99				
293.15	178.04	605.20	598.67	608.85	1239.3	614.23	2315.3	622.49
293.15	2334.3	622.49						
303.15	244.45	565.1	244.78	564.91	1402.6	574.52	2117.0	581.26
313.15	342.52	523.80	1074.1	531.05	1079.4	531.01	2184.1	541.32
323.15	457.19	483.46	1681.8	496.45	3590.7	515.64		
333.15	604.30	443.5	1716.4	456.53	2277.4	463.61		
343.15	782.31	402.53	784.2	402.64	1978.4	419.03	2000.7	419.29
353.15	998.48	361.28	2242.2	380.73				
363.15	1259.8	319.13	2753.1	348.82				
373.15	1572.08	275.96	1572.19	276.01	2348.8	294.23	2955.1	307.10

experimental data with standard deviations of $\pm 0.25\,\mathrm{kg \cdot m^{-3}}$ and $\pm 0.65\,\mathrm{kg \cdot m^{-3}}$ in the temperature ranges (314–411) K and (299–411) K for the vapor and liquid, respectively. Figure 5 shows the results of our measurements in comparison with other data [1,3]. All data for the density of the saturated vapor agree within the estimated errors. The data for the density of the saturated liquid obtained by the vibrating method [1] lie higher by 0.25–0.45% than those calculated from Eq. 6.

3.5 Speed of Sound

The speed of sound (U) for the liquid phase was measured along isotherms from 263 K to 373.15 K at increments of 10 K at pressures from P_S to 3.59 MPa. All measurements were carried out at a constant frequency of about 1.15 MHz. The results are given in Table 6. Uncertainties of the measured values did not exceed 0.05–0.1% except for the range close to the saturation line where they increased to 0.2%. Speed-of-sound measurements were not carried out in the liquid phase close to the critical point (at 383.15, 393.15, and 403.15 K) because of the intense sound absorption.

4 Conclusion

The obtained results might be useful in developing an equation of state for HFC-236ea. However, there are deviations between results of different researchers, and sometimes these discrepancies are larger than the experimental errors. The most probable reason of the apparent discrepancies is probably related to the purity (composition) of the studied samples; therefore, additional investigations of the properties of HFC-236ea are needed.

Acknowledgments We gratefully acknowledge the financial support for this research from the Siberian Branch of the Russian Academy of Sciences (Grant No.81-06) and the Russian Foundation of Basic Research (Grant No. 05-08-01173).

References

1. D.R. Defibaugh, K.A. Gillis, M.R. Moldover, J.W. Schmidt, L.A. Weber, Fluid Phase Equilib. **122**, 131 (1996)
2. K.A. Gillis, Int. J. Thermophys. **18**, 73 (1997)
3. H.L. Zhang, H. Sato, K. Watanabe, Int. J. Thermophys. **18**, 407 (1997)
4. G. Di Nicola, G. Giuliano, J. Chem. Eng. Data **45**, 1075 (2000)
5. V.A. Gruzdev, R.A. Khairulin, S.G. Komarov, S.V. Stankus, Int. J. Thermophys. **23**, 809 (2002)
6. S.G. Komarov, V.A. Gruzdev, Thermophys. Aeromech. **8**, 467 (2001)
7. S.V. Stankus, R.A. Khairulin, Int. J. Thermophys. **27**, 1110 (2006)
8. Y.Y. Duan, L. Shi, M.S. Zhu, L.Z. Han, C. Zhang, Int. J. Thermophys. **22**, 1463 (2001)
9. R.C. Reid, J.M. Prausnitz, T.K. Sherwood, *The Properties of Gases and Liquids,* 3rd edn. (McGraw-Hill, New York, 1977)
10. M.A. Anisimov, *Critical Phenomena in Liquids and Liquid Crystals* (Nauka, Moscow, 1987) [in Russian]